Aeolian processes across transverse dunes. II: Modelling the sediment transport and profile development

van Dijk, P.M.; Arens, S.M.; van Boxel, J.H.

DOI
10.1002/(SICI)1096-9837(199904)24:4<319::AID-ESP963>3.3.CO;2-D

Publication date
1999

Document Version
Final published version

Published in
Earth Surface Processes and Landforms

Earth Surface Processes and Landforms
Earth Surf. Process. Landforms **24,** 319–333 (1999)

AEOLIAN PROCESSES ACROSS TRANSVERSE DUNES. II: MODELLING THE SEDIMENT TRANSPORT AND PROFILE DEVELOPMENT

P. M. VAN DIJK, S. M. ARENS AND J. H. VAN BOXEL*

Netherlands Centre for Geo-Ecological Research ICG, Landscape and Environmental Research Group, University of Amsterdam, Nieuwe Prinsengracht 130, NL-1018 VZ Amsterdam, The Netherlands

Received 13 November 1997; Revised 18 August 1998; Accepted 17 September 1998

ABSTRACT

This paper discusses a model which simulates dune development resulting from aeolian saltation transport. The model was developed for application to coastal foredunes, but is also applicable to sandy deserts with transverse dunes. Sediment transport is calculated using published deterministic and empirical relationships, describing the influence of meteorological conditions, topography, sediment characteristics and vegetation. A so-called adaptation length is incorporated to calculate the development of transport equilibrium along the profile. Changes in topography are derived from the predicted transport, using the continuity equation. Vegetation height is incorporated in the model as a dynamic variable. Vegetation can be buried during transport events, which results in important changes in the sediment transport rates. The sediment transport model is dynamically linked to a second-order closure air flow model, which predicts friction velocities over the profile, influenced by topography and surface roughness.

Modelling results are shown for (a) the growth and migration of bare, initially sine-shaped dunes, and (b) dune building on a partly vegetated and initially flat surface. Results show that the bare symmetrical dunes change into asymmetric shapes with a slipface on the lee side. This result could only be achieved in combination with the second-order closure model for the calculation of air flow. The simulations with the partly vegetated surfaces reveal that the resulting dune morphology strongly depends on the value of the adaptation length parameter and on the vegetation height. The latter result implies that the dynamical interaction between aeolian activity and vegetation (reaction to burial, growth rates) is highly relevant in dune geomorphology and deserves much attention in future studies.

KEY WORDS aeolian sediment transport; dune dynamics; wind erosion; simulation model; vegetation; transverse dunes; coastal dunes

INTRODUCTION

In aeolian research, a fair amount of attention has been paid to theory development of isolated subprocesses of the aeolian system. Examples are effects of vegetation on air flow (Wasson and Nanninga, 1986; Buckley, 1987; Raupach, 1992; Hagen and Armbrust, 1994), effects of topography on air flow (Jackson and Hunt, 1975; Zeman and Jensen, 1987), effects of surface moisture conditions on initiation of particle movement (e.g. Chepil, 1956; Belly, 1964; Kawata and Tsuchiya, 1976; McKenna-Neuman and Nickling, 1989) and effects of slope angle on initiation of particle movement (Howard, 1977; Allen, 1982; Dyer, 1986; Hardisty and Whitehouse, 1988; Iversen and Rasmussen, 1994). The evolution of aeolian dunes is determined by many of these processes, acting simultaneously and interacting dynamically. However, few studies are dedicated to the integration of this knowledge on sediment transport processes and turbulent flow in the atmospheric boundary layer. A recent study by Stam (1997) integrates the flow model of Jackson and Hunt (1975) and a linearization of Bagnold's sediment transport equation. However, the model of Stam does not incorporate effects of vegetation on aeolian sediment transport. Other limitations are (a) the Jackson and Hunt model cannot be used to derive surface friction velocities for hills steeper than about 3° (Van Boxel *et al.*, 1999), and (b) the model

* Correspondence to: J.H. van Boxel, Netherlands Centre for Geo-Ecological Research ICG, Landscape and Environmental Research Group, University of Amsterdam, Nieuwe Prinsengracht 130, NL-1018 VZ Amsterdam, The Netherlands. Email: J.H.Boxel@frw.uva.nl
Contract/grant sponsor: Rijkswaterstaat, Ministry of Transport, Public Works and Water Management, through the TAW, the Technical Advisory Committee for Water Defences

CCC 0197-9337/99/040319–15 $17.50

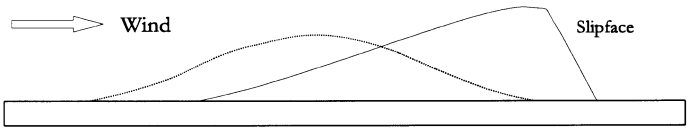

Figure 1. Under the influence of a continuous, unidirectional wind with supply of sediment from upwind areas, a symmetrically shaped body of sand develops towards a asymmetrical dune with a slipface at the lee (after Bagnold, 1954)

assumes shear stress and sediment transport to be in phase. Applied to a sine topography, the model of Stam predicts a constant dune migration rate and an exponential growth. The sine shape remains during the simulations. Simulated dune shapes do not resemble natural dune geomorphology and are inconceivable from an aerodynamical point of view. Bagnold (1954) studied the development of a symmetrical dune under the influence of a unidirectional erosive wind, with supply of sediment towards the dune (Figure 1). An asymmetrical dune develops, with a slipface at the lee. A lee slope with a slipface may trap all the sediment which is transported over the dune crest. The key to the development of such dunes is the interaction between topography and air flow and between air flow and sediment transport.

The present study integrates knowledge about several aeolian processes and compiles it into a physical model of dune profile evolution. Arens (1994) provided a conceptual model for aeolian processes in the Dutch foredunes, which is the basis of this study. The physical model utilizes well-known relationships from the literature for the quantification of effects of meteorology, topography, sediment features and vegetation on sediment transport by wind. It is dynamically linked to a second-order closure model for calculation of air flow over dunes (Van Boxel *et al.*, 1999; Zeman and Jensen, 1987). The model can be applied to various aeolian environments, including coastal foredunes, flats and transverse dunes, provided that (a) saltation is the dominant transport mode, and (b) there are no serious variations in flow directions along the considered profile (otherwise it is necessary to consider a second horizontal dimension). The latter condition implies that the model cannot be applied to complex three-dimensional topography.

As the model was developed for application to coastal foredunes, some model options specific to this environment were implemented (e.g. tide effects). These will not be dealt with here. In this paper, model concepts are discussed. The operation of the model is illustrated using two simple situations which can readily be interpreted: (a) the growth and migration of bare, initially sine-shaped dunes, and (b) dune building on partly vegetated, initially flat surfaces.

BASIC MODEL STRUCTURE

The model is designed to simulate aeolian sediment transport over ridges of sand. For the time being, the model deals only with wind perpendicular to the ridge. After reading the site data (topographic profile, its vegetation cover and sediment data) and meteorological conditions, the basic procedure followed in the model is:

(a) calculation of the air flow over the dune profile using the external air flow model, which is described in Van Boxel *et al.* (1999);
(b) calculation of the sediment transport rates along the profile;
(c) calculation of the resulting surface height changes and output of the new profile.

These steps are repeated for each time step until the end of the simulation. Thus, the wind field responds to the dune profile changes. Horizontal gradients in transport rates imply net erosion or deposition of sediment (principle of continuity):

$$\frac{\partial z(x,t)}{\partial t} = -\frac{1}{\rho_s(1-\Phi)}\left(\frac{\partial Q(x,t)}{\partial x}\right) \quad (1)$$

where z is surface elevation (m), t is time (s), ρ_s is particle density (kg m^{-3}), Φ is soil porosity (m^3 m^{-3}), $Q(x)$ is the local sediment transport in x-direction per unit length in y-direction (kg m^{-1} s^{-1}). Assuming the dry bulk density of the sand to be constant along the profile, the changes in surface height only depend on gradients in $Q(x)$. Therefore, the calculation of $Q(x)$ is the central aspect of the model. The following sections describe how local sediment transport rates are calculated and how they are affected by topography, roughness (vegetation), grain size, surface slope and surface moisture.

POTENTIAL AND ACTUAL SEDIMENT TRANSPORT

Potential transport (Q_{eq}) is the transport rate that is reached when the conditions at the location under consideration (wind, sediment, vegetation etc.) would also apply to the wide surrounding area. Several basic equations for the calculation of Q_{eq} can be found in the literature. Well known equations are those of Bagnold (1954), Kawamura (1964) and Lettau and Lettau (1977). Here, the equation of Kawamura is given as an example:

$$Q_{eq} = C_k \frac{\rho_a}{g}(U_{*s} - U_{*t})(U_{*s} + U_{*t})^2 \quad (2)$$

where Q_{eq} is the potential sediment transport rate (kg m^{-1} s^{-1}), C_k is the Kawamura constant (*c.* 2·78), ρ_a is the air density (kg m^{-3}), g is the acceleration due to gravity (m s^{-2}), U_{*s} is the surface friction velocity (m s^{-1}) and U_{*t} the threshold friction velocity for sediment transport. According to this equation, the potential sediment transport depends on the friction velocity at the surface (a measure of the erosive force) and the threshold friction velocity (a measure of the resistance of the sediment against transport). Sediment transport commences as soon as the threshold is exceeded.

Transport conditions, reflected in U_{*s} and U_{*t}, vary in time and space. As a result, the actual sediment transport rate will often differ from the potential transport rate. When transport conditions change, the transport rate adapts to the new conditions within a certain time span and within a certain distance (Kawamura, 1964; Stout, 1990; McEwan and Willetts, 1991; Butterfield, 1993). Time and distance are related to each other through the velocity of the saltating grains. Wind tunnel and modelling research has shown that equilibrium transport typically is reached in 1–2s (McEwan and Willetts, 1991; Butterfield, 1993). Our dune model is not concerned with this kind of time resolution. During saltation, the average horizontal velocity of the grains may be in the order of 2·5 to 5·0 m s^{-1} (e.g. Willetts and Rice, 1985). Thus for wind tunnel conditions, a spatial change in transport conditions may cause changing mass fluxes over a distance of about 2·5 to 10 m. Indeed, such distances are of interest at the scale of a dune. Therefore, a parameter called 'adaptation length' is being utilized in the model, which is a measure for the distance over which sediment transport adapts to a new equilibrium condition. It is similar to the length/time scale described in Butterfield (1991) and the length scale used by Anderson (1988). The expression used to assess the actual transport reads:

$$Q(x) = Q_{eq}(x) + [Q(x - \partial x) - Q_{eq}(x)]\mathrm{e}^{-\partial x/\chi} \quad (3)$$

where $Q(x)$ is the actual sediment transport rate at location x, $Q_{eq}(x)$ is the potential transport rate at x, $Q(x-\partial x)$ is the actual transport rate immediately upwind of x, and χ is the adaptation length (m).

In order to get some idea about values for the adaptation length under field conditions, several publications about spatial variations in Q were examined (e.g. Kawamura, 1964; Svasek and Terwindt,

1974; Horikawa *et al*., 1983, 1984; Hotta, 1988; Anderson, 1988; Hesp, 1989). The controls on the value of the adaptation length are still obscure. For a situation in which sediment transport increases in the downwind direction, χ was found to vary between about 6 and 13m depending on surface moisture conditions, grain size and wind speed (Kawamura, 1964; Svasek and Terwindt, 1974; Horikawa *et al*., 1983, 1984; Hotta, 1988). In the case of transport which decreases in the downwind direction, lower values are found. Anderson (1988) describes deposition patterns of wind-blown sand at the lee of aeolian dunes. Deposition rates were highest just beyond the crest and decreased exponentially further away. Anderson (1988) found the adaptation length for this process to be about 1m. On the basis of a study by Hesp (1989), it was estimated that for sand transport within regularly spaced vegetation χ is about 3m. Thus χ tends to be higher in the case of increasing transport in the downwind direction than during decreasing transport (Van Dijk, 1996). Therefore, in our model a distinction is made between χ_1 and χ_2, which are the adaptation lengths during spatially increasing and decreasing transport respectively. In this study χ_1 and χ_2 were set to 10 and 3m respectively. Evidently, further research is needed on the adaptation length parameter.

Along the profile under consideration, U_{*_s} and U_{*_t} need to be quantified (Equation 3). The surface friction velocity depends on (a) topography, which may accelerate or decelerate the air flow, (b) surface roughness due to microrelief and vegetation, and (c) the upstream friction velocity. The threshold friction velocity is determined by stabilizing forces acting on the sand grains and depends on (a) sediment characteristics, like grain size distribution, grain density and shape, (b) the local slope angle, and (c) cohesive forces between the grains. Figure 2 shows these factors and the way in which they affect sediment transport.

MODELLING SURFACE FRICTION VELOCITY

Topographic and roughness effects: the air flow model

Most aeolian environments are neither flat nor homogeneous, so the friction velocity cannot be derived from the logarithmic wind profile (Van Boxel *et al*., 1999). Surface morphology may be rather complex and multiple surface roughness transitions may be present along dune profiles. For these conditions, analytical solutions for assessing surface friction velocity are not available. Therefore, an air flow model is used for calculating wind and friction velocities as influenced by topography and surface roughness. It is based on a model of Zeman and Jensen (1987) and uses second-order closure (Stull, 1988), which means that all turbulence terms are incorporated. A full description of the air flow model is given in Van Boxel *et al*. (1999). This model needs input information on (a) the upstream friction velocity, (b) the two-dimensional topographic profile, and (c) roughness lengths along this profile. Calculated wind profiles only apply to levels at or above the aerodynamic surface. This surface is not necessarily the ground surface, for instance in the case of dense vegetation. In the case of a bare surface, the air flow model yields the surface friction velocity (U_{*_s}). Over a vegetated surface, model output relates to the friction velocity immediately above the vegetation layer (U_{*_v}).

The air flow model is not capable of dealing with recirculation vortices (Van Boxel *et al*., 1999). As a result, flow in the separation zone, often occurring in the lee of a dune, will be modelled incorrectly. The computed flow reattaches closer to the crest than expected, sometimes already on the slipface causing slipface erosion. To prevent this, a separation zone was defined, extending over a horizontal direction of five times the dune height, but only if the lee slope was steeper than 15°. This is a practical approach. However, it is important to improve on this in the air flow model itself.

Vegetation effects

Vegetation leads to an increase of the aerodynamic roughness length (z_0), and to an increase of the friction velocity above the vegetation layer (U_{*_v}). In the vegetation layer itself, momentum is extracted

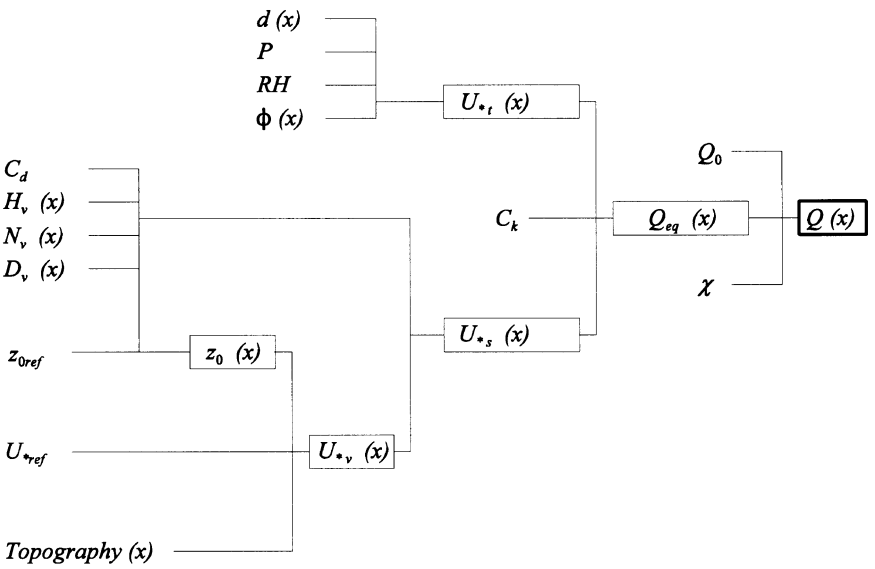

Overview of model parameters and variables

$Q(x)$	= actual sediment transport at point x	(kg·m^{-1}·s^{-1})
Variables/parameters that determine $Q(x)$:		
$Q_{eq}(x)$	= potential sediment transport at point x	(kg·m^{-1}·s^{-1})
Q_0	= sediment transport at $x = 0$	(kg·m^{-1}·s^{-1})
$U_{*t}(x)$	= threshold friction velocity at point x	(m·s^{-1})
$U_{*s}(x)$	= actual friction velocity at the surface at point x	(m·s^{-1})
χ	= adaptation length	(m)
C_k	= Kawamura constant	(-)
Variables/parameters that determine $U_{*s}(x)$:		
z-profile	= the considered (dune) profile	
$U_{*v}(x)$	= friction velocity above the vegetation layer at point x	(m·s^{-1})
U_{*ref}	= reference friction velocity (upwind of the z-profile)	(m·s^{-1})
z_{0ref}	= aerodynamic roughness length (upwind of the z-profile)	(m)
$z_0(x)$	= aerodynamic roughness length at point x	(m)
$H_v(x)$	= vegetation height at point x	(m)
$N_v(x)$	= vegetation density at point x	(m^{-2})
D_v	= average stalk diameter	(m)
C_d	= drag coefficient of the vegetation	(-)
Variables/parameters that determine $U_{*t}(x)$:		
$d(x)$	= average grain diameter at point x	(m)
RH	= relative humidity	(%)
P	= rainfall	(0/1)
$\phi(x)$	= slope angle at point x	(m·m^{-1})

Figure 2. Model parameters and variables. Spatial variables are marked by '(x)'

from the air flow and turbulence is produced at the lee side of the roughness elements (Glendening, 1977; Raupach, 1992).

The surface friction velocity (U_{*s}) depends on the vegetation physiography, and on the density and spatial configuration of the elements. Raupach (1992) derived an equation which describes the reduction of U_{*v} towards the ground. The expression reads:

$$\frac{U_{*s}}{U_{*v}} = \frac{1}{\sqrt{1+\beta\lambda}} \tag{4}$$

where β is equal to the ratio of the drag coefficient of an isolated roughness element and the drag coefficient of the underlying undisturbed surface, and λ is the roughness density or frontal plant area index ($m^2\ m^{-2}$). With β-values between 100 and 180, Equation 4 was found to agree well with data from the field and laboratory (Raupach, 1992). For simple standing stalks, λ can be determined from stalk height, diameter and density (number of stalks per unit area), using:

$$\lambda = H_v\, D_v\, N_v \tag{5}$$

where H_v is the vegetation height (m), D_v is the stalk diameter (m) and N_v is the number of stalks (m^{-2}). The value of U_{*v} in Equation 4 is derived from the external air flow model (Van Boxel *et al.*, 1999). The roughness length, which the air flow model needs as input, is calculated using the equation proposed by Hagen and Armbrust (1994):

$$z_0 = \frac{H_v}{K_1 + \dfrac{K_2\ \ln(C_d\,\lambda)}{C_d\,\lambda} + \dfrac{K_3}{C_d\,\lambda}} \quad (\lambda > 0) \tag{6}$$

with

$$\begin{aligned} K_1 &= 28{\cdot}41 - 3{\cdot}72\ \ln(D_v) \\ K_2 &= -3{\cdot}052 + 0{\cdot}6\ \ln(D_v) \\ K_3 &= -8{\cdot}33 + 1{\cdot}541\ \ln(D_v) \end{aligned} \tag{7}$$

in which D_v is stalk diameter (mm), C_d is the drag coefficient and z_0 is the aerodynamic roughness length (m).

MODELLING THE THRESHOLD FRICTION VELOCITY

The threshold friction velocity, U_{*t}, is affected by a number of factors, such as grain size and shape, particle size distribution, surface slope, sediment moisture content, rain, and crusts due to salt or algae. In our model, U_{*t} is determined from:

$$U_{*t} = U_{*t0}\, f_1(\Phi)\, f_2(RH)\, f_3(P) \tag{8}$$

Here U_{*t0} is the threshold friction velocity of a cohesionless sediment on a horizontal surface. The functions f_1, f_2 and f_3 represent the effects of surface slope, humidity and rain on the saltation threshold. Effects of crusts are not incorporated in the model. Below, the components of Equation 8 are discussed.

Particle size

According to Bagnold (1954), the threshold friction velocity of cohesionless sediment on a horizontal surface can be described by:

$$U_{*t0} = A \sqrt{\frac{\rho_s - \rho_a}{\rho_a}\, g\, d} \tag{9}$$

in which d is the average particle diameter and A is a coefficient of about 0·1 to 0·118 (Bagnold, 1954; Pye and Tsoar, 1990) for grain sizes larger than 0·1 mm.

Williams (1964), Sarre (1987) and Van der Wal *et al.* (1995) mention the effects of grain shape and sorting on U_{*t}. Grain shape was found to have significant effects only at relatively low wind speeds (Williams, 1964). The effect of sorting is rather difficult to quantify, especially because the grain size distribution of the top layer changes as a result of erosion and deposition. However, in the case of natural dune sands, having a rather uniform grain size distribution, sorting effects can be neglected (Van der Wal, 1998). Sorting and particle shape effects are not implemented in the model.

Surface slope angle

Due to gravity effects, more wind shear is necessary to move particles on positively sloping surfaces (i.e. uphill air flow), while on negative slopes sediment is mobilized more easily (Iversen and Rasmussen, 1994):

$$f_1(\Phi) = \sqrt{cos\Phi + \frac{sin\Phi}{tan\alpha}} \tag{10}$$

where Φ is the surface slope angle (degrees) and α is the angle of repose. If $\Phi = 0$, then $U_{*t\Phi}$ and U_{*t0} are equal. If $\Phi = \alpha$, sediment will start to move spontaneously and a slipface will develop. However, on the slipface the main transport mechanism is not aeolian transport, but avalanching. This process cannot be modelled on the basis of the sediment transport equation, which deals with aeolian transport. Therefore, we decided to implement a separate avalanching routine. In this routine, sediment is redistributed along the slope as soon as the slope angle exceeds the angle of yield (*c.* 37°). This is an iterative process which continues until the slope angle is less than or equal to the angle of repose (*c.* 33°).

Cohesion and rainfall

Cohesion between particles increases surface resistance and therefore U_{*t}. Cohesion may result from the presence of moisture, salt, algae, clay, organic matter and carbonate. So far, our model only accounts for moisture effects. An equation for salt effects is available from Nickling and Ecclestone (1981).

In many aeolian studies, the dominant role of surface moisture is stressed (Chepil, 1956; Belly, 1964; McKenna-Neuman and Nickling, 1989; Bradley *et al.*, 1992; Van Dijk *et al.*, 1996; Arens, 1996). Moisture increases the resistance of the sand particles against lift and drag, due to cohesive forces of the adsorbed water films surrounding them. Namikas and Sherman (1994) compared several models which describe the relationship between surface moisture content and U_{*t}. With these models an average increase of 48 per cent in U_{*t} was calculated if the gravimetric moisture content increased from 0 to 0·6 per cent. However, the variation in the predicted increase was very large: values varied between 4 and 105 per cent. At a higher moisture content (4 per cent), the predicted increase varied between 47 and 206 per cent. These are substantial differences. Surface moisture content is highly dynamic, shows high spatial variations and is difficult to measure. At present, application of such models to field situations is hardly possible. Therefore, our model uses an alternative approach which is based on the influence of air humidity on the surface moisture content. For rainless days, Arens (1996) found:

$$f_2(RH) = \left(1 - \frac{K}{100} + \frac{K}{100 - RH}\right) \tag{11}$$

in which RH is the relative humidity (per cent) and K is a coefficient (2·11). RH is easy to measure and well documented in meteorological databases. It can be used as a dynamic input variable in order to model U_{*t} dynamically, without having to deal with evaporation rate calculations. This equation does not hold in situations where (or on days when) surface moisture is dominated by other sources such as rainfall (see below), tidal water or ground water. This approach also does not allow for spatial variations in surface moisture.

The effects of rainfall on sediment transport by wind are twofold (Van Dijk *et al.*, 1996): (a) intensive wind-driven rain can transport sediment by combined splash and saltation processes; (b) residual moisture increases the cohesive forces between particles and therewith the resistance of the sediment against lift and drag. On a sand beach in The Netherlands, the first process was shown to be significant over short time intervals during high-intensity rain events (De Lima *et al.*, 1992). However, this study also indicated that sediment transport by wind during rainfall is, in terms of quantity, of secondary importance, and thus not relevant for dune development. Therefore, this process is not incorporated in the model. The effect of residual moisture resulting from rainfall lasts over longer time spans and was studied by Arens (1996). On average, rainy days yielded U_{*t}-values 35 per cent higher than on those on dry days, so:

$$f_3(P) = 1 + C_r \tag{12}$$

where C_r is a coefficient (0 on dry days and 0·35 on rainy days).

RESULTS AND DISCUSSION

Here, we present some applications of the model to illustrate its features and possibilities. Results of two simulation series are shown: the first deals with the vertical growth and migration of unvegetated sine-shaped sand dunes; the second is about dune building on an initially flat surface due to the presence of vegetation. The air flow model (Van Boxel *et al.*, 1999) was called every time a critical change in height (dz_{crit}) was detected somewhere in the profile. In all simulations, sediment input into the system at $x = 0$ was set equal to the potential transport. Furthermore, a deflation limit (z-value) was defined below which further erosion is not possible (e.g. groundwater level or a non-erodible layer).

Series 1: vertical growth and migration of bare, initially sine-shaped dunes

In this series, the growth and migration of isolated unvegetated sand dunes overlying a flat unerodable surface were studied. Simulations were carried out with different initial dune heights between 1 and 10 m. The base width was the same for all dunes and they were all symmetrically sine-shaped at $t = 0$. The average particle diameter was set to 200 μm. The dunes were exposed to a moderately erosive wind ($U_{*ref} = 0{\cdot}33\,\mathrm{m\ s^{-1}}$, which is 1·5 times the threshold of $0{\cdot}22\,\mathrm{m\ s^{-1}}$). The time step was about 15 min and the distance step was 0·8 m. In most cases, the simulation period was 100 days.

As an example, Figure 3 shows the simulation results for the 1 and 6 m dunes. If we consider the entire simulation series, the symmetrical shape of all dunes changes into an asymmetrical shape with a slipface at the lee side. These results compare rather well with the development shown in Figure 1. Furthermore, all dunes gain height. After some time a maximum dune height is reached which remains approximately constant until the end of the simulation (Figure 4a). The higher the initial dune, the sooner this maximum is reached. The lower dunes (e.g. the 2 m dune in Figure 4a) do not reach a stable height within 100 days. The differences in growth rates are due to the fact that wind accelerations and decelerations are stronger in the case of higher and steeper topography. This results in stronger sediment transport gradients along the dune crest and in higher deposition rates.

As soon as the dune has developed a slipface, all sediment that is transported along the stoss slope is

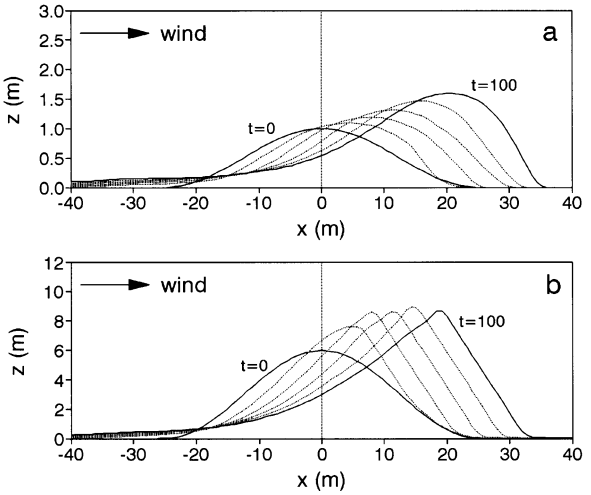

Figure 3. The simulated evolution of unvegetated, initially sine-shaped dunes with supply of sediment from upwind areas, under the influence of a unidirectional moderately erosive wind during 100 days. $U_{*ref} = 0{\cdot}33\text{m s}^{-1}$, $U_{*t0} = 0{\cdot}22\text{m s}^{-1}$. The initial dune heights are (a) 1m and (b) 6m

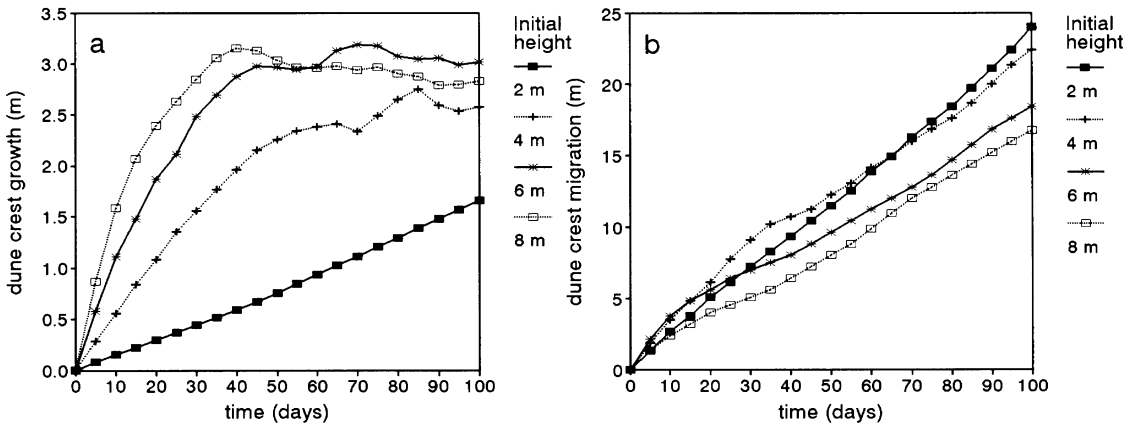

Figure 4. Modelled vertical growth (a) and migration (b) of unvegetated, initially sine-shaped dunes, with supply of sediment from upwind areas under the influence of a unidirectional moderately erosive wind. $U_{*ref} = 0{\cdot}33\text{m s}^{-1}$, $U_{*t0} = 0{\cdot}22\text{m s}^{-1}$

deposited at the lee of the dune. The shape of the stoss slope continues to adjust gradually, while the slope length increases. The migration rate of the dune crest is lower for the higher dunes (see Figure 4b, the 6 and 8m dunes). Because these dunes have longer lee slopes, more sediment deposition is needed to produce a certain migration distance. The migration rates of the 2 and 4m dunes are less different. During the first 60 days, the 4m dune migrates even faster than the 2m dune. This is due to the fact that it takes such a long time for the 2m dune to develop a slipface. Thus, compared to the 4m dune, the 2m dune traps less sediment, resulting in a reduction of the migration rate.

The simulations show that the dunes develop towards a dynamic equilibrium in which vertical growth is negligible as the dune migrates at constant speed. Further growth can only be achieved by disturbance of this equilibrium. Disturbances can be caused in many ways, but variations in wind directions are probably most important. The impact of changing wind directions on dune evolution is illustrated by a

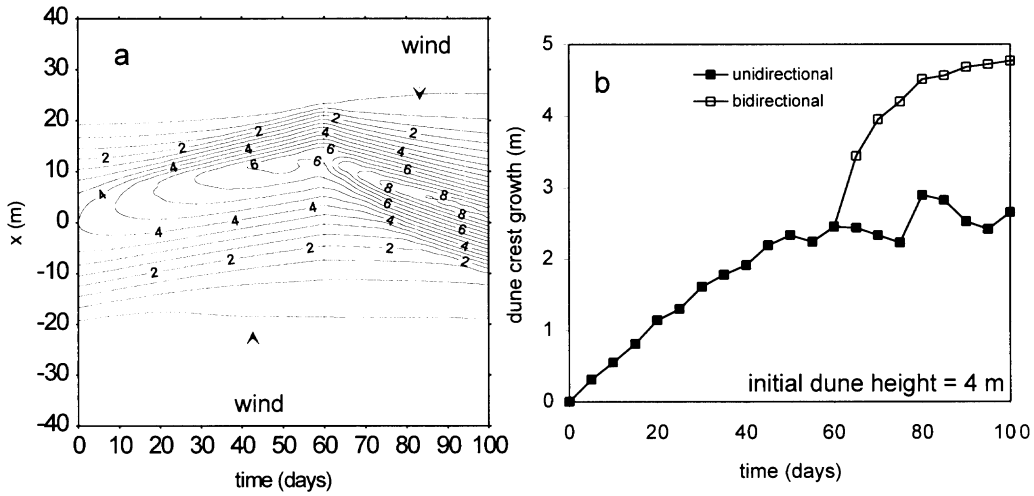

Figure 5. The effect of variable wind directions on simulated dune morphology (a) and vertical growth (b). The initial dune height is 4m. During the first 60 days the wind blows in the direction of increasing x. After that time, the wind comes from the opposite direction

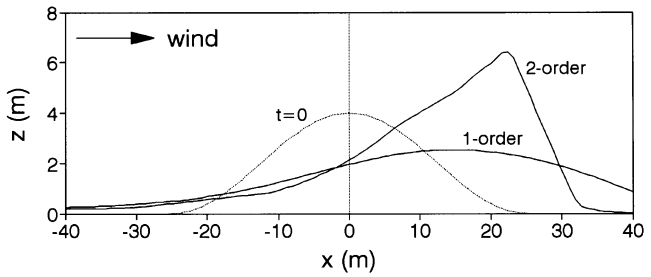

Figure 6. Modelled dune evolution after 100 days, using a first-order closure air flow model and a second-order closure model

simulation in which the wind direction changes to the opposite direction on $t = 60$ days (Figure 5a). During the first 60 days, the dune crest has reached a stable height. As soon as the wind changes direction, a sharp decline in transport occurs at the dune crest causing it to gain height. Again the growth decreases in time (Figure 5b). This example shows that winds with changing directions can induce the formation of relatively high dunes. Unidirectional winds are less effective in doing that.

It appears that some essential features of developed unvegetated dunes can only be modelled if turbulence terms and particularly streamline curvature effects are explicitly included in the air flow calculations. This became apparent when we linked the transport model to a first-order closure air flow model instead of the second-order closure model. When using the first-order closure model, there was no slipface development and all dunes lost height (Figure 6). Van Boxel *et al.* (1999) explain the role of streamline curvature with respect to vertical dune growth: streamline curvature causes a reduction in the surface friction velocity at the dune crest, even though measured wind speeds at some height above the crest often show strong speed-up. As a result, bare dunes can grow in height. Earlier, Wiggs *et al.* (1996) stressed the significance of streamline curvature on aeolian processes at the stoss slope of dunes.

The importance of the dynamic interaction between air flow and topography for dune development is shown in Figure 7. Here, crest growth and migration in time are shown for different values of dz_{crit}, which is the critical height change in the dune profile for air flow recalculation. The higher the value of

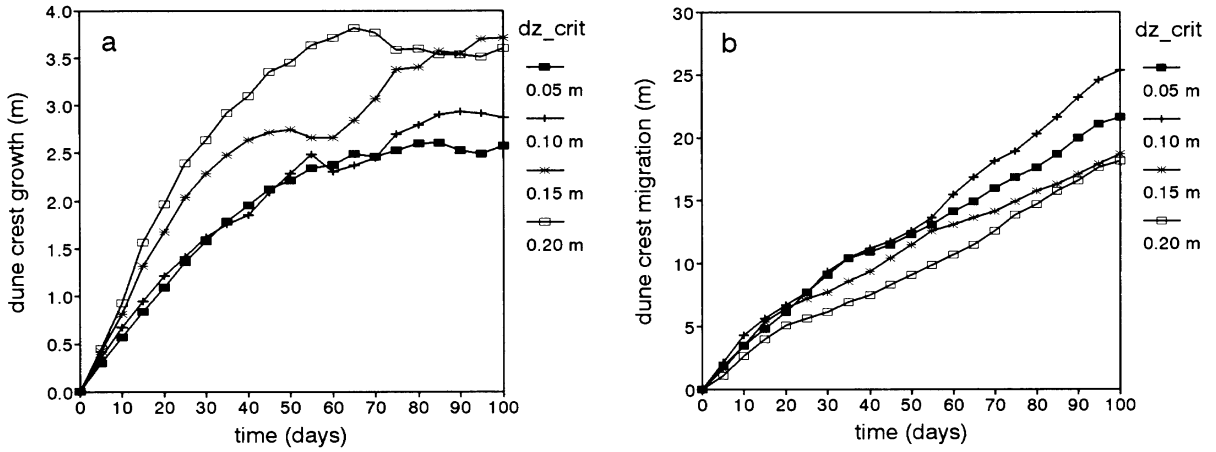

Figure 7. The sensitivity of modelled growth in dune height (a) and migration (b) to the frequency of air flow recalculation (the higher dz_crit, the less frequently air flow is recalculated). The initial dune height is 4m

dz_{crit}, the less frequently air flow is recalculated. It was found that modelling results became poor when using dz_{crit} above 0·12m (Figure 7). So, the critical value chosen is important: if too high, the model will generate implausible morphological features; if too low, the calculation time may increase significantly.

How do the computed dune profiles compare to real-world transverse dune profiles? This paper does not go into model validation, which is the next phase of this research. Here, a few figures of modelled dunes are compared with figures mentioned in the literature. Modelled lee slope angles with slipfaces agree with literature data and are all close to 33°. Figure 8a shows the development of stoss slope angles for initial dune heights of 3 and 9m over a 300-day simulation period. Initially, the slope of the 9m dune is steep and far from steady-state. The angle gradually decreases and approaches the stoss slope angle of the 3m dune. This adjustment takes quite a long time. For both dunes, the model predicts a steady-state slope angle of 7 to 8°. According to Livingstone and Warren (1996), most transverse dunes have stoss slope angles between 5 and 10°. Lancaster (1995) mentions windward slope angles of 2–3° at the toe, 10–12° in the middle and again 2–3° at the upper part of the slope for simple crescentic and barchanoid ridges. Hesp and Hastings (1998) found stoss slope angles between 4 and 11° along the centreline axis of barchan dunes, and that of the barchan which was studied by Lancaster *et al.* (1996) was 7·1°. Thus, modelled stoss slopes angles are within the right range. The height of the two dunes seems to converge towards a value of about 11m (Figure 8b). The 9m dune adjusts its height very rapidly, because of the high transport gradients at the dune crest. The 3m dune gradually builds up its height and keeps a rather constant stoss slope angle during this process. The initial height/width ratios were 0·18 (9m dune) and 0·06 (3m dune). At the end of the simulation, the ratio approaches 0·11 for both dunes. For barchans, Lancaster (1995) mentions a ratio of 0·1 and in Hesp and Hastings (1998) the values range from 0·06 to 0·10. Data on oblique dunes (Hunter *et al.*, 1983) showed a ratio of 0·11 (average height and width are 25m and 225m respectively).

Series 2: dune building on partly vegetated, initially flat surfaces

In this series, the initial situation is a horizontal, flat surface which is partly vegetated. Sediment ($d = 200\mu m$) is transported towards the vegetated surface where deposition takes place and a dune starts to develop. Vegetational, meteorological and sedimentological parameters were varied over a wide range of values. The simulation period was four days and vegetation growth was assumed to be negligible. However, vegetation height is a dynamic variable in this series due to sediment deposition.

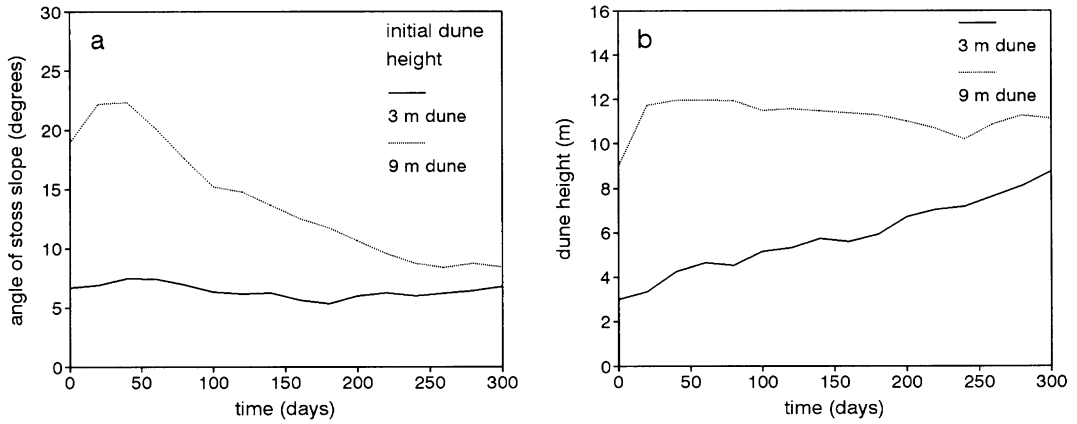

Figure 8. Modelled development of stoss slope angles (a) and crest height (b) for unvegetated, initially sine-shaped dunes with supply of sediment from upwind areas, under the influence of a unidirectional wind during 300 days. $U_{*ref} = 0{\cdot}33\text{m s}^{-1}$, $U_{*t0} = 0{\cdot}22\text{m s}^{-1}$

The result of this series shows that two groups of parameters/variables can be distinguished. The first group largely determines the overall sediment transport intensity (upstream friction velocity, grain size, rainfall and the relative air humidity belong to this group); the second dominates the spatial patterns in transport rates and thus erosion/deposition patterns. Here we discuss only two parameters of the second group. From the first simulation series it is clear that topography itself is a very important factor affecting transport gradients and thus belongs to the second group of parameters. The present simulation series shows that vegetation height and the adaptation length also determine spatial transport patterns to a large extent (Figure 9).

With respect to the adaptation length, higher values cause smoother transport gradients and as a result, a smoother topography (Figure 9A). The model results are most sensitive to variations of the adaptation length in the range between 0 and 6m. The dune, developing due to the presence of vegetation, affects the air flow, therewith inducing additional vertical dune growth. As a result, the dune height exceeds that of the vegetation.

Simulation results for different vegetation heights are shown in Figure 9B. The surface with low vegetation gets covered with smooth sheets of sediment, burying a large part of the vegetated surface. The surface with higher vegetation shows a distinct depositional ridge in the first few metres of vegetation, but much less deposition occurs further downwind. These results are supported by field observations (Arens and Deiller, 1996).

CONCLUSIONS

In this paper, we have shown that it is possible to simulate dune shapes which have morphological features that are consistent with those of natural dunes. In order to achieve this, it is necessary to use a second-order closure model for the calculation of air flow. Turbulent variations in the air flow have a significant influence on the pattern of surface friction velocities and consequently on sediment transport patterns. These patterns are unpredictable if turbulence terms and streamline curvature effects are neglected.

In unvegetated sandy environments, the interaction between topography and air flow and the interaction between air flow and sediment transport processes largely determines the morphological evolution. According to the model, under unidirectional wind regimes, dunes appear to develop towards a dynamic equilibrium in which further vertical growth is negligible and the dune crest migration rate is constant. Winds with changing directions can induce the formation of high dunes.

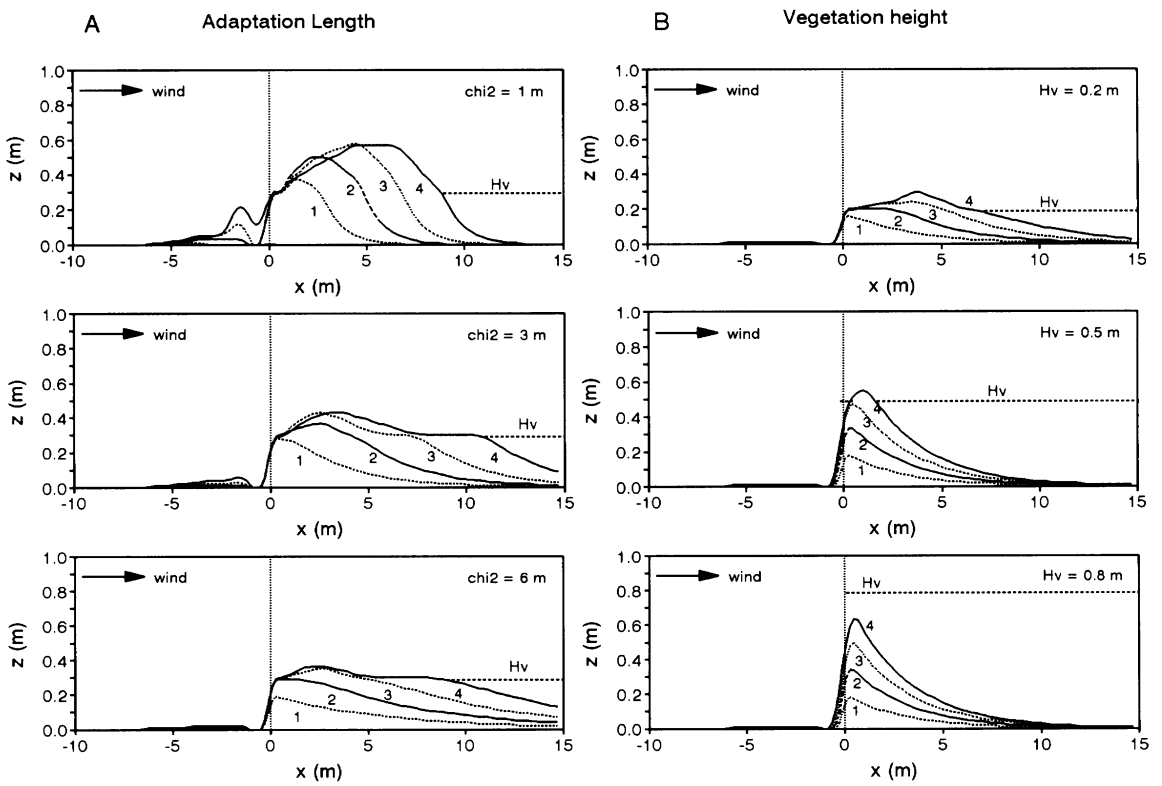

Figure 9. Modelled dune development on a partly vegetated surface (initially flat) during four days under the influence of a constant wind ($U_{*ref} = 0{\cdot}4$m s^{-1}) for (A) three different values of the adaptation length ($\chi_2 = 1$, 3 and 6m) and (B) three different vegetation heights (Hv = 0·2, 0·5 and 0·8m, $\chi_2 = 3$m). Vegetation is present downwind of $x = 0$

In vegetated environments, the vegetation cover and physiography and its response to aeolian activity dominate the dune development. Vegetation height largely determines the morphological features of the depositional landforms that develop. Therefore, the dynamic interaction between aeolian activity (sediment deposition rate, scouring) and vegetation (reaction to burial, growth rates) is highly relevant in dune geomorphology and deserves much attention in future studies.

The coupled models for air flow and aeolian sediment transport can be valuable tools to improve our understanding of dune dynamics. In this paper, a few possibilities have been presented. Obviously, the model can be used to investigate many more aspects of dune dynamics. However, before doing that, it is necessary to achieve model validation. This will be the next step in this research. Once validated, the model can be used by dune managers to compare the effects of various managing/control options on dune morphology. Besides the validation, work has to be done on model improvement. Concerning the air flow model, the problem of flow separation was mentioned by Van Boxel *et al.* (1999). The sediment transport model may need to be improved on the determination of the adaptation length parameter, to which modelling results were shown to be fairly sensitive.

ACKNOWLEDGEMENTS

This work is part of the project 'Physical Modelling of Foredune Development', which is supported financially by Rijkswaterstaat, Ministry of Transport, Public Works and Water Management, through the TAW, the Technical Advisory Committee for Water Defences. This support is gratefully acknowledged. Ir H. J. Verhagen, dr ir H. Steetzel, ir A. P. de Looff and ir J. van der Kolff, all

members of the Advisory Board, are thanked for their contributions throughout the project. We thank two anonymous reviewers for their valuable comments on the manuscript.

REFERENCES

Allen, J. R. L. 1982. 'Simple models for the shape and symmetry of tidal sand waves: (1) statically stable equilibrium forms', *Marine Geology,* **48**, 31–49.
Anderson, R. A. 1988. 'The pattern of grainfall deposition in the lee of aeolian dunes', *Sedimentology,* **35**, 175–188.
Arens, S. M. 1994. *Aeolian processes in the Dutch foredunes*, Thesis, University of Amsterdam, The Netherlands, 150 pp.
Arens, S. M. 1996. 'Rates of aeolian transport on a beach in a temperate humid climate', *Geomorphology,* **17**, 3–18.
Arens, S. M. and Deiller, A.-F. 1996. 'Monitoring van een grootschalige verstuiving Van Limburg Stirum gebied, Amsterdamse Waterleiding Duinen. Vastlegging uitgangssituatie', Landscape and Environmental Research Group, University of Amsterdam.
Bagnold, R. A. 1954. *The Physics of Blown Sand and Desert Dunes*, 2nd edition, Metheun, London.
Belly, P.-Y. 1964. *Sand movement by wind*, US Army Corps of Engineers, Coastal Engineering Research Center, Technical Memo No. **1**, Washington, DC.
Bradley, N. W., Gregory, J. M. and Wilson, G. R. 1992. 'Wet-bonding effects on threshold friction velocity', *American Society of Agricultural Engineers, Winter Meeting*, Nashville, TN, paper no. 922515.
Buckley, R. 1987. 'The effect of sparse vegetation on the transport of dune sand by wind', *Nature,* **325**, 426–428.
Butterfield, G. R. 1991. 'Grain transport rates in steady and unsteady turbulent flows', *Acta Mechanica, Suppl.* **1**, 97–122.
Butterfield, G. R. 1993. 'Sand transport response to fluctuating wind velocity', in Clifford, N. J., French, J. R. and Hardisty, J. (Eds), *Turbulence, Perspectives on Flow and Sedinment Transport*, 305–335.
Chepil, W. S. 1956. 'Influence of soil moisture on erodibility of soil by wind', *Soil Science Society of America Proceedings,* **20**, 288–292.
De Lima, J. L. M. P., Van Dijk, P. M. and Spaan, W. P. 1992. 'Splash-saltation transport under wind-driven rain', *Soil Technology,* **5**, 151–166.
Dyer, K. R. 1986. *Coastal and Estuarine Sediment Dynamics*, Wiley, New York.
Glendening, J. W. 1977. *Aeolian transport and vegetation capture of particles*, Thesis, Colorado State University.
Hagen, L. J. and Armbrust, D. V. 1994. 'Plant canopy effects on wind erosion saltation', *Transactions of the American Society of Agricultural Engineers,* **37**, 461–465.
Hardisty, J. and Whitehouse, R. J. S. 1988. 'Evidence for a new sand transport process from experiments on Saharan dunes', *Nature,* **325**, 426–428.
Hesp, P. A. 1989. 'A review of biological and geomorphological processes involved in the initiation and development of incipient foredunes', in Gimingham, C. H., Ritchie, W., Willetts, B. B. and Willis, A. J. (Eds), *Coastal Sand Dunes, Proceedings Royal Society Edinburgh,* **96B**, 181–201.
Hesp, P. A. and Hastings, K. 1998. 'Width, height and slope relationships and aerodynamic maintenance of barchans', *Geomorphology,* **22**, 193–204.
Horikawa, K., Hotta, S., Kubota, S. and Katori, S. 1983. 'On the sand transport rate by wind on a beach', *Coastal Engineering in Japan,* **26**, 101–120.
Horikawa, K., Hotta, S., Kubota, S. and Katori, S. 1984. 'Field measurement of blown sand transport rate by trench trap', *Coastal Engineering in Japan,* **27**, 213–232.
Hotta, S. 1988. 'Sand transport by wind', in Horikawa, K. (Ed.), *Nearshore Dynamics and Coastal Processes*, Part II, University of Tokyo, Japan, 218–238.
Howard, A. D. 1977. 'Effect of slope on threshold of motion and its application to orientation of wind ripples', *Geological Society of America Bulletin,* **88**, 853–856.
Hunter, R. E., Richmond, B. M. and Alpha, T. R. 1983. 'Storm-controlled oblique dunes of the Oregon coast', *Geological Society of America Bulletin,* **94**, 1450–1465.
Iversen, J. D. and Rasmussen, K. R. 1994. 'Effect of slope on saltation threshold', *Sedimentology,* **41**, 721–728.
Jackson, O. S. and Hunt, J. C. R. 1975. 'Turbulent flow over a low hill', *Quarterly Journal of the Royal Meteorological Society,* **101**, 925–955.
Kawamura, R. 1964. *Study of sand movement by wind*, Hydraulic Engineering Laboratory Technical Report, **HEL-2–8**, University of California, Berkely, 99–108.
Kawata, Y. and Tsuchiya, Y. 1976. 'Influence of water content on the threshold of sand movement and the rate of sand transport in blown sand', *Proceedings Japanese Society of Civil Engineers,* **249**, 95–100.
Lancaster, N. 1995. *Geomorphology of Desert Dunes*, Routledge, London.
Lancaster, N., Nickling, W. R., McKenna Neuman, C. K. and Wyatt, V. E. 1996. 'Sediment flux and airflow on the stoss slope of a barchan dune', *Geomorphology,* **17**, 55–62.
Lettau, K. and Lettau, H. 1977. 'Experimental and micro-meteorological field studies of dune migration', in Lettau, K. and Lettau, H (Eds), *Exploring the World's Driest Climate*, IES Report **101**, University of Wisconsin Press, Madison, 110–147.
Livingstone, I. and Warren, A. 1996. *Aeolian Geomorphology. An Introduction*, Longman, Singapore, 211 pp.
McEwan, I. K. and Willetts, B. B. 1991. 'Numerical model of the saltation cloud', *Acta Mechanica,* **1**. 53–66.
McKenna-Neuman, C. and Nickling, W. G. 1989. 'A theoretical and wind tunnel investigation of the effect of capillary water on the entrainment of sediment', *Canadian Journal of Soil Science,* **69**, 79–96.
Namikas, L. M. and Sherman, D. J. 1994. 'A review of the effects of surface moisture content on aeolian sand transport, in Tchakerian, V. (Ed.), *Desert Aeolian Processes*, Chapman and Hall, London.

Nickling, W. G. and Ecclestone, M. 1981. 'The effects of soluble salts on the threshold shear velocity of fine sand', *Sedimentology,* **28**, 505–510.
Pye, K. and Tsoar, H. 1990. *Aeolian Sand and Sand Dunes*, Unwin Hyman, London.
Raupach, M. R. 1992. 'Drag and drag partition on rough surfaces', *Boundary Layer Meteorology,* **60**, 375–395.
Sarre, R. D. 1987. 'Aeolian sand transport', *Progress in Physical Geography,* **11**, 157–182.
Stam, J. M. T. 1997. 'On the modelling of two-dimensional aeolian dunes', *Sedimentology,* **44**, 127–141.
Stout, J. E. 1990. 'Wind erosion within a simple field', *Transactions of the American Society of Agricultural Engineers,* **33**, 1597–1600.
Stull, R. B. 1988. *An Introduction to Boundary Layer Climatology*, Kluwer Academic Publishers, Dordrecht, 666 pp.
Svasek, J. N. and Terwindt, J. H. J. 1974. 'Measurements of sand transport by wind on a natural beach', *Sedimentology,* **21**, 311–322.
Van Boxel, J. H., Arens, S. M., Van Dijk, P. M. 1999. 'Aeolian processes across transverse ridges. I: Modelling the air flow', *Earth Surface Processes and Landforms*
Van der Wal, D. 1998. 'The impact of the grain-size distribution of nourishment sand on aeolian sediment transport', *Journal of Coastal Research,* **14**, 620–631.
Van der Wal, D., Peters, B. A. M., Putten, W. H. van der, and Tongeren, O. F. R. 1995. *Inventariserend onderzoek naar de ecologische effecten van zandsuppleties*, University of Amsterdam, Netherlands Institute of Ecology, for Rijkswaterstaat, 115 pp.
Van Dijk, P. M. 1996. *Modellering zandtransport zeereep. Aanpassingslengtes, vegetatie en modelgevoeligheid*, University of Amsterdam, for Rijkswaterstaat (TAWC), 53 pp.
Van Dijk, P. M., De Lima, J. L. M. P. and Stroosnijder, L. 1996. 'The influence of rainfall on transport of beach sand by wind', *Earth Surface Processes and Landforms,* **21**, 341–352.
Wasson, R. J. and Nanninga, P. M. 1986. 'Estimating wind transport of sand on vegetated surfaces', *Earth Surface Processes and Landforms,* **11**, 505–514.
Wiggs, G. F. S., Livingstone, I. and Warren, A. 1996. 'The role of streamline curvature in sand dune dynamics: evidence from field and wind tunnel measurements', *Geomorphology,* **17**, 29–46.
Willetts, B. B. and Rice, M. A. 1985. 'Inter-saltation collisions', in Barndorff-Nielsen, O. E. *et al., Proceedings of International Workshop on Physics of Blown Sand*, Memoirs, **8**, 83–100.
Williams, G. 1964. 'Some aspects of the eolian saltation load', *Sedimentology,* **3**, 257–287.
Zeman, O. and Jensen, N. O. 1987. 'Modifications of turbulence characteristics in flow over hills', *Quarternary Journal of the Royal Meteorological Society,* **113**, 55–80.

